



Published in final edited form as:

Heart Rhythm. 2014 June ; 11(6): 1063–1069. doi:10.1016/j.hrthm.2014.03.021.

Optimizing CRT to Minimize ATP Consumption Heterogeneity Throughout the Left Ventricle: A Simulation Analysis Using a Canine Heart Failure Model

Yuxuan Hu, MSE*, Viatcheslav Gurev, PhD^{*.1}, Jason Constantino, PhD*, and Natalia Trayanova, PhD FHRs*

*Department of Biomedical Engineering, Johns Hopkins University, Baltimore, Maryland, USA

Abstract

Background—Cardiac resynchronization therapy (CRT) has been demonstrated to lead to the restoration of oxygen consumption homogeneity throughout the left ventricle (LV), which is important for long-term reverse remodeling of the ventricles. However, research has focused exclusively on identifying the LV pacing sites that led to acute hemodynamic improvements. It remains unclear whether there exist LV pacing sites that could both improve the hemodynamics and result in ATP consumption homogeneity throughout the LV, thus maximizing both CRT short-term and long-term benefits.

Objective—We aimed to demonstrate the feasibility of optimizing CRT pacing locations to achieve maximal improvement in both ATPCTHI (an ATP consumption heterogeneity index) and stroke work.

Methods—We employed an MRI-based electromechanical model of the dyssynchronous failing (DHF) canine ventricles. ATPCTHI and stroke work improvement were determined for each of 34 CRT pacing sites evenly spaced over the LV epicardium.

Results—Results demonstrated the feasibility of determining the optimal LV pacing site that achieves simultaneous maximum improvements in ATPCTHI and stroke work. The optimal LV CRT pacing sites in the DHF canine ventricles were located midway between apex and base. The improvement in ATPCTHI decreased more rapidly with the distance from the optimal sites as compared to stroke work improvement. CRT from the optimal sites homogenized ATP consumption by increasing septal ATP consumption and decreasing that of the lateral wall.

Conclusion—Simulation results using a canine heart failure model demonstrated that CRT can be optimized to achieve improvements in both ATPCTHI and stroke work.

© 2014 The Heart Rhythm Society. Published by Elsevier Inc. All rights reserved.

Corresponding author: Natalia Trayanova, Biomedical Engineering Department, Johns Hopkins University, Hackerman Hall 216, 3400 North Charles Street, Baltimore MD 21218, (410)516-4375, ntrayanova@jhu.edu.

¹Dr Viatcheslav Gurev's current address is Multiscale Systems Biology and Modeling Group, IBM T.J. Watson Research Center, Yorktown Heights, NY, USA

Publisher's Disclaimer: This is a PDF file of an unedited manuscript that has been accepted for publication. As a service to our customers we are providing this early version of the manuscript. The manuscript will undergo copyediting, typesetting, and review of the resulting proof before it is published in its final citable form. Please note that during the production process errors may be discovered which could affect the content, and all legal disclaimers that apply to the journal pertain.

Keywords

Heart failure; Cardiac resynchronization therapy; Dyssynchronous heart failure; Left bundle branch block; Reverse remodeling; Optimal pacing site

Introduction

Heart failure is a major cause of morbidity and mortality,¹ contributing significantly to global health expenditure. A large number of heart failure patients exhibit contractile dyssynchrony due to left bundle branch block (LBBB); in these patients, the contraction of the left ventricle (LV) is delayed compared to that of the right ventricle (RV).^{2, 3} Cardiac resynchronization therapy (CRT), the administering of biventricular pacing to the ventricles to re-coordinate contraction, has proven to be an effective therapy for dyssynchronous heart failure (DHF) patients.⁴⁻⁶

In DHF patients, as a result of contractile dyssynchrony, the myocardial blood flow (a measure of myocardial workload) and oxygen consumption is higher in the LV lateral wall compared to the septum.⁷ Over the long term, the LV lateral wall mass increases to a greater extent relative to the septal mass, i.e. an asymmetry in the hypertrophic response develops.⁸ CRT has been demonstrated to lead to the restoration of relative homogeneity in oxygen consumption throughout the LV by increasing the oxygen consumption of the septum and decreasing that of the lateral wall.^{7, 9} Homogeneous oxygen consumption, which indicates uniform distribution of myocardial workload, throughout the LV is important for long-term reverse remodeling of the ventricles as it eliminates the asymmetry in hypertrophy resulting from LBBB.⁸

Consequentially, an important consideration in the quest to improve the long-term efficacy of CRT for DHF patients is that oxygen (or ATP) consumption heterogeneity throughout the LV be minimized. However, thus far research into CRT has not addressed this issue -- previous studies have mainly focused on improving the acute response of CRT.¹⁰ Indeed, only the optimal LV pacing sites that give rise to acute hemodynamic improvements, such as stroke work increase, have been identified.¹⁰ It therefore remains unclear whether there exist LV pacing sites that could both improve the acute hemodynamic response and result in a relatively homogeneity of ATP consumption throughout the LV, thus maximizing both short-term and long-term benefits of CRT.

The goal of the present study was to address this issue. We aimed to demonstrate the feasibility of optimizing CRT pacing locations to achieve minimal ATP consumption heterogeneity throughout the LV while simultaneously maximizing hemodynamics improvement in the DHF canine ventricles. A magnetic resonance image (MRI)-based electromechanical model of the DHF canine ventricles previously developed by us was augmented and used to achieve the study goals.

Materials and Methods

MRI-based electromechanical model of the DHF ventricles

We employed an MRI-based electromechanical model of the DHF canine ventricles (Fig. 1A) developed previously by our group.^{11, 12} The model, as previously published, is briefly described in the online Supplemental Methods. For the present research, we implemented further advancements in the model to enable us to determine the ATP consumption throughout the LV at a high spatiotemporal resolution. Detailed description of these new model developments is also provided in Supplemental Methods.

CRT Simulation protocol

Currently, in a routine clinical CRT device implantation procedure, LV pacing sites are accessed via the coronary sinus and are thus epicardial.¹³ Accordingly, the model of the DHF ventricles was subjected to bi-ventricular CRT, in which the ventricles were paced simultaneously from the RV apex and an epicardial location in the LV. This protocol is similar to the CRT protocol described in our recent publication.¹² The parameters chosen in the CRT model, such as CRT AV delay and pacing rate are provided in the Supplemental Methods. To determine the optimal epicardial LV CRT pacing locations that result in minimum ATP consumption heterogeneity throughout the LV while simultaneously maximizing stroke work improvement, 34 evenly spaced LV epicardial pacing sites were tested (Fig. 1B, left). For each LV pacing site, maps of the distribution of ATP_{cT}, the ATP consumption per myosin head (see Supplemental Methods for detail), were constructed, and a single ATP_{cT} heterogeneity index heterogeneity index, ATPCTHI, calculated (see Supplemental Methods for detail).

In addition, we also simulated bi-ventricular CRT with endocardial LV placement to gain insight into whether it could lead to different improvements in ATPCTHI and stroke work as compared to epicardial LV placement. Three LV endocardial pacing sites were tested: one basal, one apical and one midway between apex and base (Fig. 1B, right). Improvements in both ATPCTHI and stroke work were calculated for each of them. In all CRT simulations, the position of the RV pacing lead remained the same.

Data analysis

For each bi-ventricular CRT simulation (corresponding to each of the 34 epicardial LV and the 3 endocardial LV pacing locations), the degree of heterogeneity in ATP consumption throughout the LV and the improvement in ATPCTHI was determined.

These novel calculations are described in detail in the Supplemental Methods. Additionally, the optimal LV pacing site(s), both epicardial (among 34 locations) and endocardial (among 3 locations) that led to maximal improvement in stroke work were calculated as described in our previous publication¹² and briefly presented in the Supplemental Methods. Finally, the LV pacing sites that achieve maximal improvement in both ATPCTHI and stroke work were identified.

Results

Figure 2A presents contraction in the model of the DHF canine ventricles. The black and red lines are the strain profiles over one pacing cycle from representative sites, one on the LV lateral wall and another on the septum. It can be seen that contraction is dyssynchronous: the septal wall shortened while the LV lateral wall was pre-stretched; the lateral wall contraction was delayed relative to that of the septum. These strain profiles are consistent with experimental recordings in the DHF ventricles¹⁴ and with the simulated strain maps in our previous publication.¹² Figure 2B shows the 3D distribution of ATP_cT in the DHF canine ventricles: ATP_cT was larger in the LV lateral wall compared to the septum, resulting in an ATPCTHI of 0.327.

Simulations of biventricular CRT were executed to determine the epicardial LV location that resulted in maximum improvement in ATPCTHI following CRT. First, for all 34 LV CRT locations, ATP_cT maps were constructed. Then, the ATPCTHI values, one for each CRT simulation, were determined. The left image of Fig. 3A is a summary plot of the results of all 34 simulations; it presents the distribution of the improvement in ATPCTHI (normalized with respect to the maximal improvement in ATPCTHI, 20%) over all pacing sites. Both apical and basal pacing sites gave rise to small (<10%) improvement in ATPCTHI (i.e. <50% improvement in ATPCTHI normalized with respect to the maximal improvement in ATPCTHI, as seen in Fig. 3A, left). The pacing site that resulted in maximal improvement in ATPCTHI was located midway between apex and base, and is marked by the black triangle. CRT from this LV pacing location homogenized ATP_cT between the septum and the lateral wall by increasing septal ATP_cT while decreasing that of the lateral wall (Fig. 3B, right), resulting in an ATPCTHI of 0.259.

To provide a reference value, we also calculated ATPCTHI for the failing ventricles in sinus rhythm; the activation patterns corresponding to sinus rhythm, LBBB, and CRT from the optimal pacing site are shown in Figure 4. The ATPCTHI in sinus rhythm was 0.268, slightly larger than that (0.259) following CRT from the LV location that resulted in maximal improvement in ATPCTHI.

Simulations of biventricular CRT were then conducted to determine the epicardial LV location that resulted in maximum stroke work improvement. Figure 3B is a summary plot of the results of all 34 simulations, each corresponding to one LV site; it shows the distribution of stroke work improvement (normalized with respect to the maximal stroke work improvement, 41%) over all pacing sites. Almost all of the pacing sites (33 out of 34) led to 33% stroke work improvement (i.e. 80% stroke work improvement normalized with respect to the maximal stroke work improvement as seen in Fig. 3B).

The pacing site that gave rise to the maximal stroke work improvement was located midway between apex and base (marked by the black triangle). The corresponding pressure-volume loop for this CRT location and its comparison to the pressure-volume loop in LBBB are presented in Supplemental Results and Discussion.

The pacing site that resulted in maximal improvement in ATPCTHI was adjacent to the one that led to maximal stroke work improvement and thus, CRT from both LV pacing sites

(optimal sites) resulted in maximal or near maximal improvement in both ATPCTHI and stroke work. Figure 5 is a plot showing the number of CRT LV pacing sites that gave rise to improvement above a certain level in both ATPCTHI and stroke work as a function of that level. It shows how close to the maximal improvements in ATPCTHI (20%) and stroke work (41%) the CRT responses from epicardial pacing sites were. For instance, the number of the LV pacing sites that led to improvements in both ATPCTHI and stroke work that were above 40% of the maximum possible was 25. In other words, 25 of the 34 pacing sites resulted in above 8% improvement in ATPCTHI (40% of the maximum 20% improvement in ATPCTHI is 8% improvement) and above 16% stroke work improvement (40% of the maximum 41% improvement in stroke work is 16% stroke work improvement). Similarly, the number of LV pacing sites that led to improvements in both ATPCTHI and stroke work above 80% of maximal was only 10; i.e. 10 LV pacing sites had above 16% improvement in ATPCTHI (80% of the maximum 20% improvement in ATPCTHI is 16% improvement) and above 33% stroke work improvement (80% of the maximum 41% improvement in stroke work is 33% stroke work improvement).

We also examined the mechanisms by which pacing sites midway between apex and base lead to larger improvement in ATPCTHI. To conduct this analysis, the 3D distributions of ATP_cT in the DHF canine ventricles and following CRT from a basal pacing site, an apical site, and the site that resulted in maximal improvement in ATPCTHI, were compared (Fig. 6). Six sites that were on the same longitudinal cross-section (3 on the lateral wall and 3 on the septum, indicated by the arrows in the leftmost image of the 2nd row in Fig. 6) were chosen for strain and ATP_c profile analysis. The 3rd and 4th rows of Figure 6 present the strain and ATP_c profiles over one representative pacing cycle at each of the six sites in the DHF ventricles and following CRT from the respective LV locations (broken lines are traces from the 3 sites in the septum and solid lines are traces from the 3 sites in the lateral wall). Comparing the strain profiles from the DHF ventricles and following CRT from the LV site that resulted in maximal improvement in ATPCTHI, it can be seen that there is a delay in the lateral wall contraction relative to the septal contraction in the DHF ventricles (onsets of lateral wall and septal contractions are indicated by the arrows). CRT eliminated this dyssynchrony in ventricular contraction, leading to similar ATP_c profiles between septum and lateral wall, and thus significant decrease in ATP_cT heterogeneity throughout the LV and improvement in ATPCTHI (20%).

The basal and apical CRT LV pacing sites shown in Fig. 6 resulted in an ATPCTHI of 0.304 and 0.321, respectively; normalized improvements in ATPCTHI were 34% and 8%, respectively. Pacing the LV from the base resulted in the apex contracting after the base, with the apex being pre-stretched (indicated by the arrow, green solid line in the 2nd row panel in Fig. 6) while the base was contracting; the pre-stretch was substantial (14%) as the wall of the apex was thinner than that of the base. This led to fast apical myofiber shortening during the subsequent contraction, as myofibers at the apex shortened to the same degree as those at the base but starting from a fiber pre-stretch of 14%. Consequently, there was higher ATP_c (4th row, basal pacing column) and ATP_cT (2nd row, basal pacing column) at the apex relative to those at the base. Pacing the LV from the apex led to the apex contracting ahead of the base, which resulted in dissimilar ATP_c profiles throughout the LV (4th row, apical pacing column).

Finally, we conducted bi-ventricular endocardial LV CRT simulations. The results demonstrated that the improvements in ATPCTHI were 13% (basal site), 4% (apical site) and 17% (the site midway between apex and base). The maximal improvement in ATPCTHI among the three endocardial pacing sites was 17%, which was close to the maximal improvement in ATPCTHI among the epicardial pacing sites (20%). Apical and basal pacing sites led to smaller improvement in ATPCTHI compared to the pacing site midway between apex and base. The improvements in stroke work were 36% (basal site), 39% (apical site) and 38% (the site midway between apex and base) respectively. Similar to the epicardial pacing sites, all endocardial pacing sites gave rise to stroke work improvement above 33%.

Discussion

Our study demonstrated the feasibility of determining the optimal LV pacing site for biventricular CRT that achieves simultaneous maximum improvements in ATPCTHI and stroke work. The results were based on the use of an MRI-based electromechanical model of the DHF canine ventricles. Major findings of the study include:

1. The optimal epicardial LV pacing site for biventricular CRT that resulted in maximal improvement in ATPCTHI was located midway between apex and base, and close to the site that resulted in maximal stroke work improvement.
2. The further the distance on the epicardium from a given LV pacing site to the optimal LV pacing locations, the smaller the improvement in ATPCTHI. Improvement in ATPCTHI decreased much more rapidly with this distance as compared to stroke work improvement.
3. CRT from the optimal epicardial LV pacing sites homogenized ATP_{cT} throughout the LV by increasing septal ATP_{cT} and decreasing that of the lateral wall. CRT from epicardial apical or basal sites led to the apex or base contracting ahead of the distant myocardium at base or apex. As a result, CRT from both apical and basal sites gave rise to dissimilar ATP_c profiles throughout the LV, which resulted in heterogeneous ATP_{cT} in the LV.
4. The location of the endocardial LV CRT pacing site that resulted in maximal improvement in ATPCTHI (among the three sites tested) was in the same general region of the ventricle as the optimal epicardial pacing site.

CRT-induced improvement in ATPCTHI and stroke work

To determine the oxygen consumption throughout the LV, clinical studies had employed ¹¹C-acetate positron emission tomography.^{7,9} However, these studies provided information with low temporal and spatial resolution: myocardial oxygen consumption was measured by the acetate clearance rate at every minute; the LV myocardial wall was divided into four 4 regions (anterior, lateral, inferior and septal wall) and oxygen consumption was quantified for each of them. By using a computational approach to cardiac electromechanics, we were able to evaluate, in 3D and at a high spatiotemporal resolution, the metabolic rate throughout the LV following biventricular CRT, for both epicardial and endocardial LV

pacing locations. Our MRI-based 3D electromechanical model of the failing canine ventricles incorporated a myofilament model representing ATP consumption, which made it possible to calculate the dynamic temporal changes in ATP consumption and its heterogeneous distribution throughout the LV. Thus, the LV pacing site that led to maximal improvement in ATPCTHI following CRT could be accurately determined; such CRT optimization could not be achieved in the clinical studies using ^{11}C -acetate positron emission tomography. Analyzing the mechanisms, we found in the present study that the LV pacing site that gave rise to the maximal improvement in ATPCTHI was located midway between apex and base. CRT from non-optimal sites (apical or basal) led to the apex or base contracting ahead of the distant myocardium at base or apex, resulting in dissimilar ATP_c profiles throughout the LV and thus heterogeneous ATP_cT in the LV.

In this study, we demonstrated that stroke work improvement decreased slowly with the distance from the optimal pacing location, which is in agreement with experimental evidence.^{10, 12} The slow decrease reflected the fact that our model of CRT was tuned to achieve maximum stroke work improvement (see Supplemental Results and Discussion) as the AV delay used here (70ms) was the value shown to lead to significant stroke work improvement in a canine DHF model.¹²

Clinical significance

The results of our study could have important implications for optimizing the clinical procedure of CRT. Our study demonstrated the feasibility of using an image-based simulation approach to determine the optimal LV pacing site for biventricular CRT in the DHF ventricles, a site that achieves simultaneous maximum improvements in ATPCTHI and stroke work. We demonstrated that in the tachycardia-paced canine DHF ventricles (i.e. ventricles without ischemic cardiomyopathy) the optimal LV pacing site was located midway between apex and base (based on extensive simulations of epicardial pacing CRT and a limited number of endocardial CRT simulations). However, we do not expect that in all patients the LV pacing site that maximizes improvements in both ATPCTHI and stroke work would necessarily be at that location. Indeed, clinical studies have shown that there is a significant interindividual variability in the location of the optimal LV pacing site.¹⁵⁻¹⁷ The significant interindividual variability in the location of the optimal LV pacing sites found in these clinical studies is due to the fact that a significant percentage of patients had ischemic cardiomyopathy (25%, 56% and 36% in the studies by Asbach et al.,¹⁵ Khan et al.,¹⁶ and Duckett et al.,¹⁷ respectively); the location of scar tissue influences the location of the optimal CRT pacing site.¹⁶ The image-based simulation approach to CRT optimization presented here could be applied to each patient heart, building a personalized model (with ischemic cardiomyopathy also accounted for, should there be any) to be used in determining the optimal LV pacing site (either epi- or endocardial) in a patient-specific manner.

A finding with important clinical implication is that acute hemodynamic response does not necessarily predict long-term CRT outcome, which is consistent with the results from clinical studies (see review¹⁸). Duckett et al. found that acute response to CRT, as measured by maximal rise in LV pressure, is predictive of long-term response.¹⁷ However, this study defined long-term response only in terms of reduction in LV end-systolic volume, which is

only one component of reverse remodeling. Elimination of asymmetry in hypertrophy resulting from LBBB, as examined here, is a different, in fact poorly explored, aspect of reverse remodeling by CRT.

Limitations

A limitation in our model is that because of the weak electromechanical coupling in the model we could not represent pacing-induced electro-mechanical remodeling, namely the prolongation of APD in the late-activated myocardial segment as compared to the early-activated myocardial segment found in experimental studies;^{19, 20} one expects that such electromechanical remodeling might affect the location of the LV pacing site that maximizes improvements in ATPCTHI. As more sophisticated electromechanical models are implemented in the future, the spatial heterogeneity in APD could be taken into account in calculating the optimal pacing site that will result in maximal improvements in ATPCTHI and stroke work following the approach developed here. Another limitation is that the electromechanical model did not incorporate papillary muscles. It is possible that when modeling advances enough to be able to handle the contribution of papillary muscle, the optimal LV pacing site might be found to be closer to the apex, as found in some experiments.¹⁰

Conclusion

In the present study, we demonstrated the feasibility of determining the optimal LV pacing site for biventricular CRT that achieves simultaneous maximum improvements in ATPCTHI and stroke work. In the tachycardia-paced DHF canine ventricles these optimal CRT LV pacing sites were located midway between apex and base. Our study suggests an ATP based method to optimize the location of the LV pacing sites for biventricular CRT. Prospective testing would be needed to confirm the feasibility of this method in animal models or patients.

Supplementary Material

Refer to Web version on PubMed Central for supplementary material.

Acknowledgments

This work was funded by National Institutes of Health (NIH) grants DP1-HL123271 and R01-HL103428, National Science Foundation Grants CBET-0933029 and IOS-1124804 to Natalia Trayanova, and by NIH fellowship F31-HL103090 to Jason Constantino. Natalia Trayanova is a cofounder of CardioSolv, LLC. CardioSolv was not involved in this research.

Abbreviations

| | |
|-------------------------|--|
| ATP_c | ATP consumption per myosin head |
| ATP_{cT} | total ATP _c over one pacing cycle |
| ATPCTHI | ATP _{cT} heterogeneity index |
| AV delay | atrioventricular delay |

| | |
|--------------|---|
| CRT | cardiac resynchronization therapy |
| DHF | dyssynchronous heart failure |
| DTMRI | diffusion tensor magnetic resonance image |
| LBBB | left bundle branch block |
| LV | left ventricle |
| MRI | magnetic resonance image |
| RV | right ventricle |

References

1. Lloyd-Jones D, Adams R, Carnethon M, et al. Heart disease and stroke statistics--2009 update: a report from the American Heart Association Statistics Committee and Stroke Statistics Subcommittee. *Circulation*. Jan 27.2009 119:e21–181. [PubMed: 19075105]
2. Grines CL, Bashore TM, Boudoulas H, Olson S, Shafer P, Wooley CF. Functional abnormalities in isolated left bundle branch block. The effect of interventricular asynchrony. *Circulation*. Apr.1989 79:845–853. [PubMed: 2924415]
3. Wyndham CR, Smith T, Meeran MK, Mammanna R, Levitsky S, Rosen KM. Epicardial activation in patients with left bundle branch block. *Circulation*. Apr.1980 61:696–703. [PubMed: 6444558]
4. Abraham WT, Fisher WG, Smith AL, et al. Cardiac resynchronization in chronic heart failure. *N Engl J Med*. Jun 13.2002 346:1845–1853. [PubMed: 12063368]
5. Auricchio A, Stellbrink C, Sack S, Block M, Vogt J, Bakker P, Huth C, Schondube F, Wolfhard U, Bocker D, Krahnefeld O, Kirkels H. Long-term clinical effect of hemodynamically optimized cardiac resynchronization therapy in patients with heart failure and ventricular conduction delay. *J Am Coll Cardiol*. Jun 19.2002 39:2026–2033. [PubMed: 12084604]
6. Cazeau S, Leclercq C, Lavergne T, Walker S, Varma C, Linde C, Garrigue S, Kappenberger L, Haywood GA, Santini M, Bailleul C, Daubert JC. Effects of multisite biventricular pacing in patients with heart failure and intraventricular conduction delay. *N Engl J Med*. Mar 22.2001 344:873–880. [PubMed: 11259720]
7. Lindner O, Vogt J, Kammeier A, Wielepp P, Holzinger J, Baller D, Lamp B, Hansky B, Korfer R, Horstkotte D, Burchert W. Effect of cardiac resynchronization therapy on global and regional oxygen consumption and myocardial blood flow in patients with non-ischaeamic and ischaemic cardiomyopathy. *European heart journal*. Jan.2005 26:70–76. [PubMed: 15615802]
8. Vernooy K, Cornelussen RN, Verbeek XA, Vanagt WY, van Hunnik A, Kuiper M, Arts T, Crijns HJ, Prinzen FW. Cardiac resynchronization therapy cures dyssynchronopathy in canine left bundle-branch block hearts. *European heart journal*. Sep.2007 28:2148–2155. [PubMed: 17611254]
9. Lindner O, Sorensen J, Vogt J, Fricke E, Baller D, Horstkotte D, Burchert W. Cardiac efficiency and oxygen consumption measured with ¹¹C-acetate PET after long-term cardiac resynchronization therapy. *Journal of nuclear medicine: official publication, Society of Nuclear Medicine*. Mar.2006 47:378–383.
10. Helm RH, Byrne M, Helm PA, Daya SK, Osman NF, Tunin R, Halperin HR, Berger RD, Kass DA, Lardo AC. Three-dimensional mapping of optimal left ventricular pacing site for cardiac resynchronization. *Circulation*. Feb 27.2007 115:953–961. [PubMed: 17296857]
11. Constantino J, Hu Y, Trayanova NA. A computational approach to understanding the cardiac electromechanical activation sequence in the normal and failing heart, with translation to the clinical practice of CRT. *Prog Biophys Mol Biol*. Oct-Nov;2012 110:372–379. [PubMed: 22884712]
12. Hu Y, Gurev V, Constantino J, Trayanova N. Efficient preloading of the ventricles by a properly timed atrial contraction underlies stroke work improvement in the acute response to cardiac resynchronization therapy. *Heart Rhythm*. Dec.2013 10:1800–1806. [PubMed: 23928177]

13. Bristow MR, Saxon LA, Boehmer J, Krueger S, Kass DA, De Marco T, Carson P, DiCarlo L, DeMets D, White BG, DeVries DW, Feldman AM. Cardiac-resynchronization therapy with or without an implantable defibrillator in advanced chronic heart failure. *N Engl J Med*. May 20.2004 350:2140–2150. [PubMed: 15152059]
14. Breithardt OA, Stellbrink C, Herbots L, Claus P, Sinha AM, Bijnens B, Hanrath P, Sutherland GR. Cardiac resynchronization therapy can reverse abnormal myocardial strain distribution in patients with heart failure and left bundle branch block. *J Am Coll Cardiol*. Aug 6.2003 42:486–494. [PubMed: 12906978]
15. Asbach S, Hartmann M, Wengenmayer T, Graf E, Bode C, Biermann J. Vector selection of a quadripolar left ventricular pacing lead affects acute hemodynamic response to cardiac resynchronization therapy: a randomized cross-over trial. *PloS one*. 2013; 8:e67235. [PubMed: 23826245]
16. Khan FZ, Virdee MS, Palmer CR, Pugh PJ, O'Halloran D, Elsik M, Read PA, Begley D, Fynn SP, Dutka DP. Targeted left ventricular lead placement to guide cardiac resynchronization therapy: the TARGET study: a randomized, controlled trial. *J Am Coll Cardiol*. Apr 24.2012 59:1509–1518. [PubMed: 22405632]
17. Duckett SG, Ginks M, Shetty AK, Bostock J, Gill JS, Hamid S, Kapetanakis S, Cunliffe E, Razavi R, Carr-White G, Rinaldi CA. Invasive acute hemodynamic response to guide left ventricular lead implantation predicts chronic remodeling in patients undergoing cardiac resynchronization therapy. *J Am Coll Cardiol*. Sep 6.2011 58:1128–1136. [PubMed: 21884950]
18. Prinzen FW, Auricchio A. The “missing” link between acute hemodynamic effect and clinical response. *Journal of cardiovascular translational research*. Apr.2012 5:188–195. [PubMed: 22090350]
19. Jeyaraj D, Wan X, Ficker E, Stelzer JE, Deschenes I, Liu H, Wilson LD, Decker KF, Said TH, Jain MK, Rudy Y, Rosenbaum DS. Ionic bases for electrical remodeling of the canine cardiac ventricle. *Am J Physiol Heart Circ Physiol*. Aug 1.2013 305:H410–419. [PubMed: 23709598]
20. Jeyaraj D, Wilson LD, Zhong J, Flask C, Saffitz JE, Deschenes I, Yu X, Rosenbaum DS. Mechanoelectrical feedback as novel mechanism of cardiac electrical remodeling. *Circulation*. Jun 26.2007 115:3145–3155. [PubMed: 17562957]

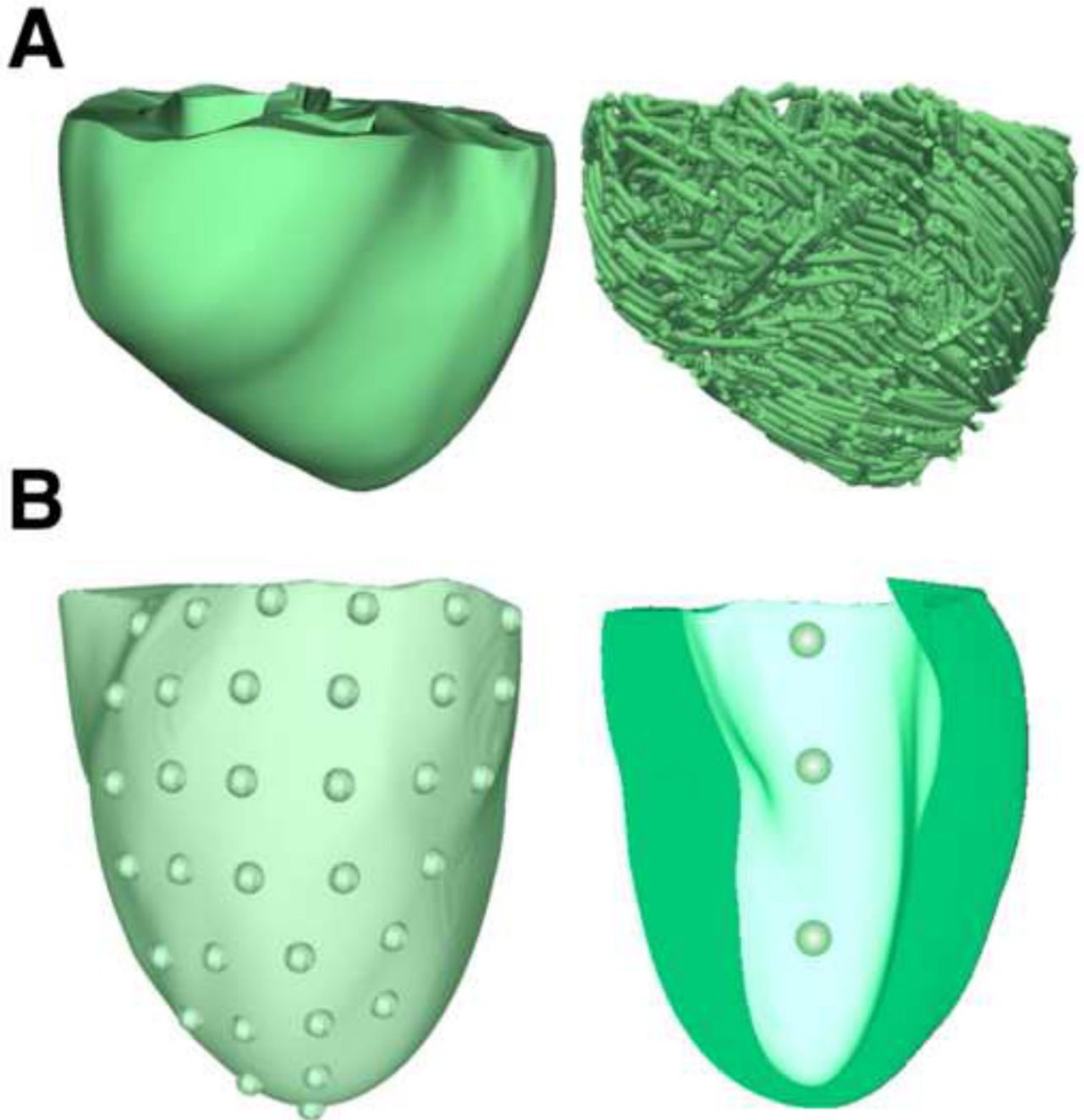


Figure 1.

(A): Geometry (left) and fiber orientation (right) of the DHF canine ventricular model. (B): Distribution of 34 evenly spaced LV epicardial pacing sites (left). The view was adjusted to show only the LV lateral wall, as most of the LV pacing sites were located on the lateral wall. Distribution of the 3 LV endocardial pacing sites (right) in a visual rendering of the LV endocardium.

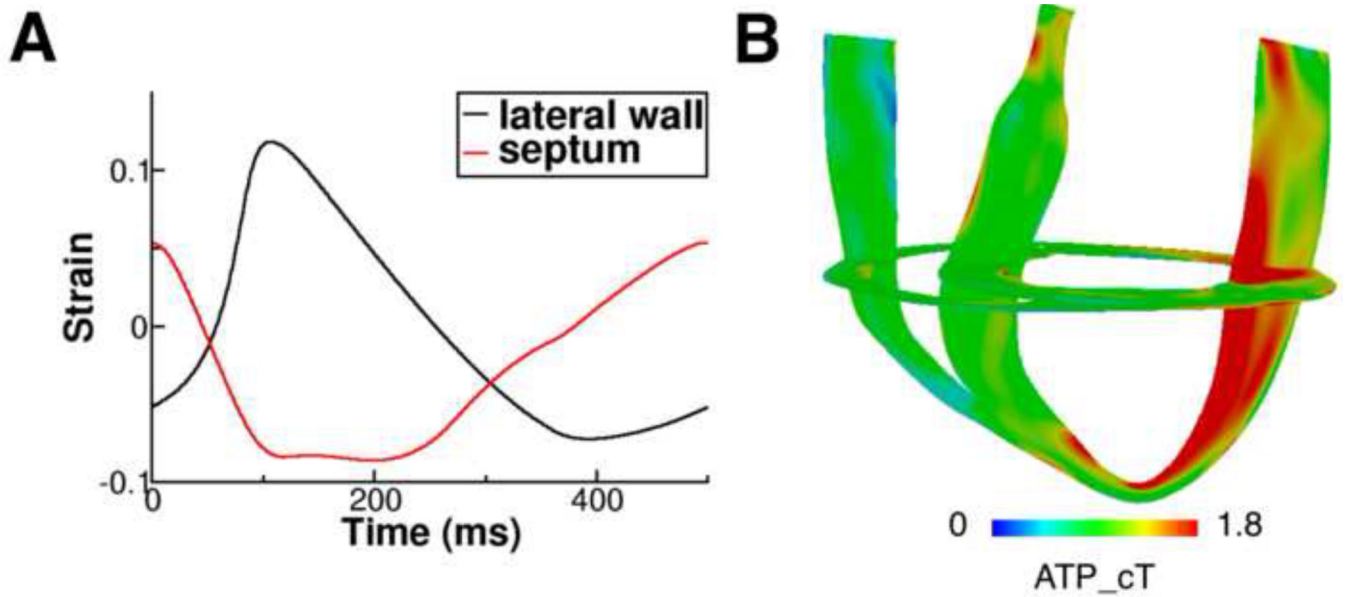


Figure 2.

(A): Strain profiles over one pacing cycle from representative sites, one on the LV lateral wall and another on the septum in the DHF canine ventricular model with simulated LBBB electrical activation. (B): 3D distribution of ATP_cT in the DHF canine ventricles.

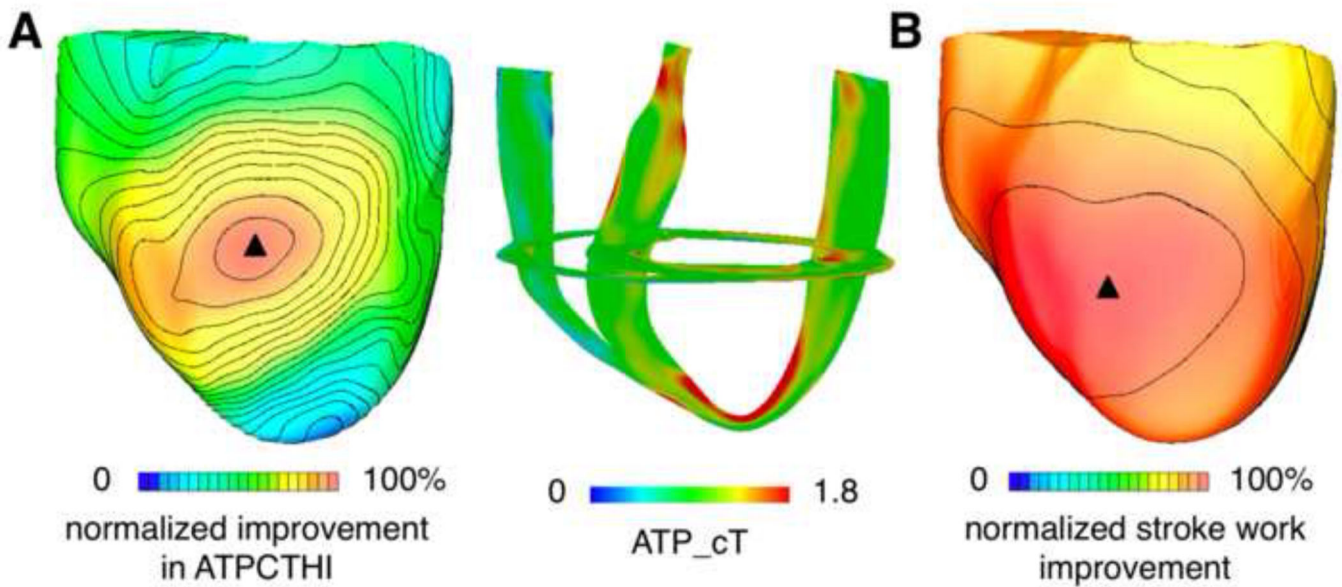


Figure 3.

(A): Distribution of improvement in ATPCTHI over all epicardial LV pacing sites for biventricular CRT (left). Improvement in ATPCTHI was normalized with respect to the maximal improvement in ATPCTHI; the value of the maximal amount of improvement in ATPCTHI was determined among the 34 CRT simulation results (corresponding to the 34 LV epicardial pacing sites). The range 0 to 100% was chosen here for the purpose of comparing isochrones between panels A and B. 3D distribution of ATP_cT in the ventricles following CRT from the epicardial LV site that resulted in maximal improvement in ATPCTHI (right). (B): Distribution of stroke work improvement over all epicardial LV pacing sites for biventricular CRT. Stroke work improvement for each of the 34 LV pacing sites was normalized with respect to the maximal stroke work improvement; the value of the maximal stroke work improvement was determined among the 34 sets of CRT simulation results.

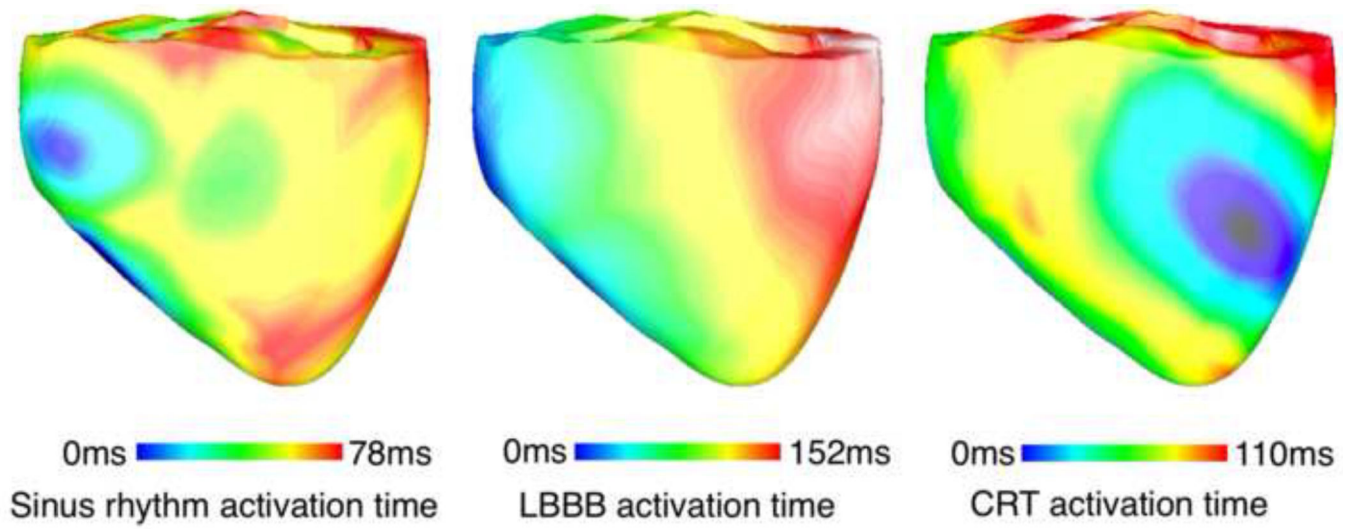


Figure 4. Electrical activation pattern in the canine ventricles corresponding to sinus rhythm, LBBB, and CRT from the optimal endocardial LV pacing site.

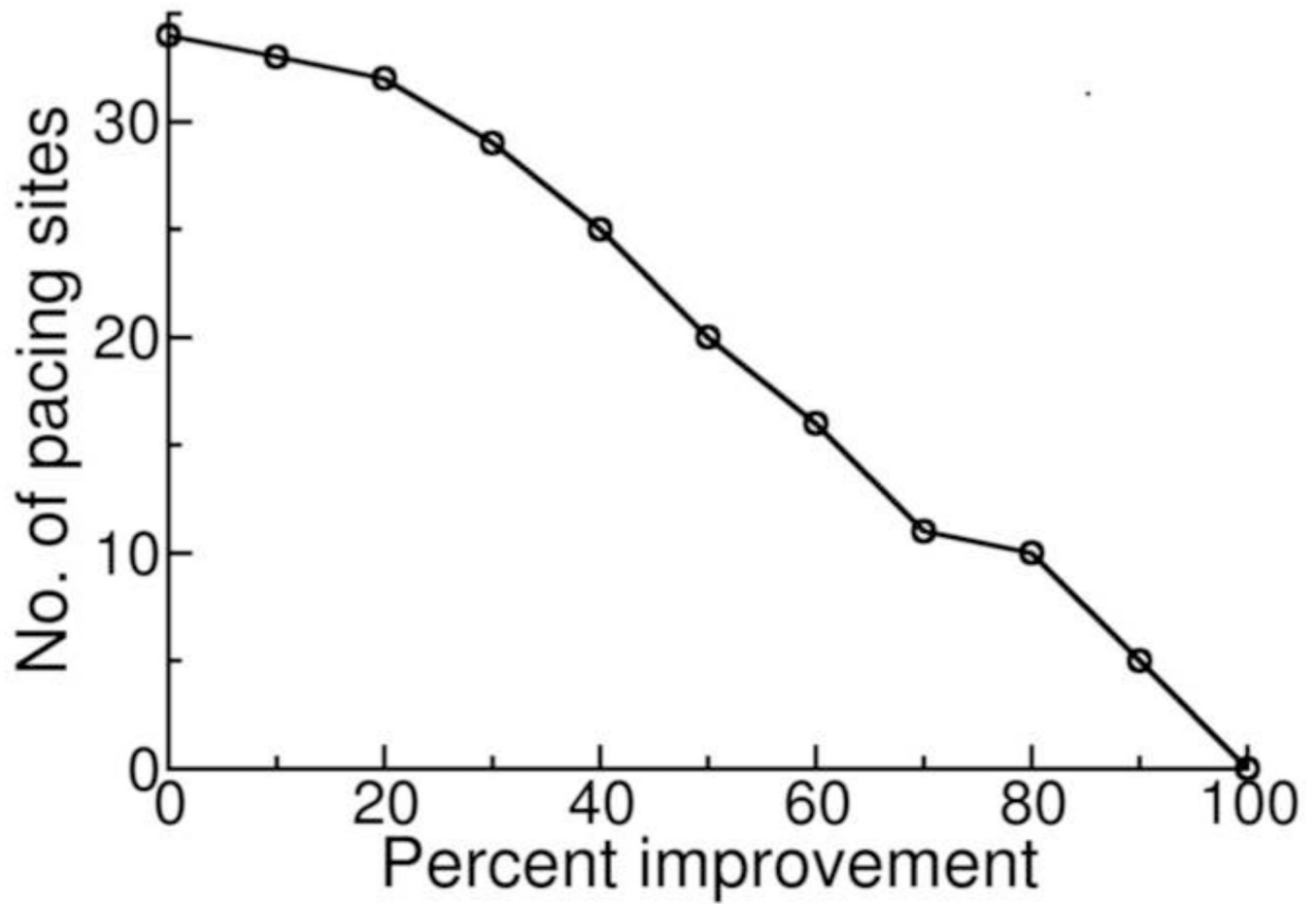


Figure 5. The number of CRT LV pacing sites that gave rise to improvement above a certain level in both ATPCTHI and stroke work as a function of that level.

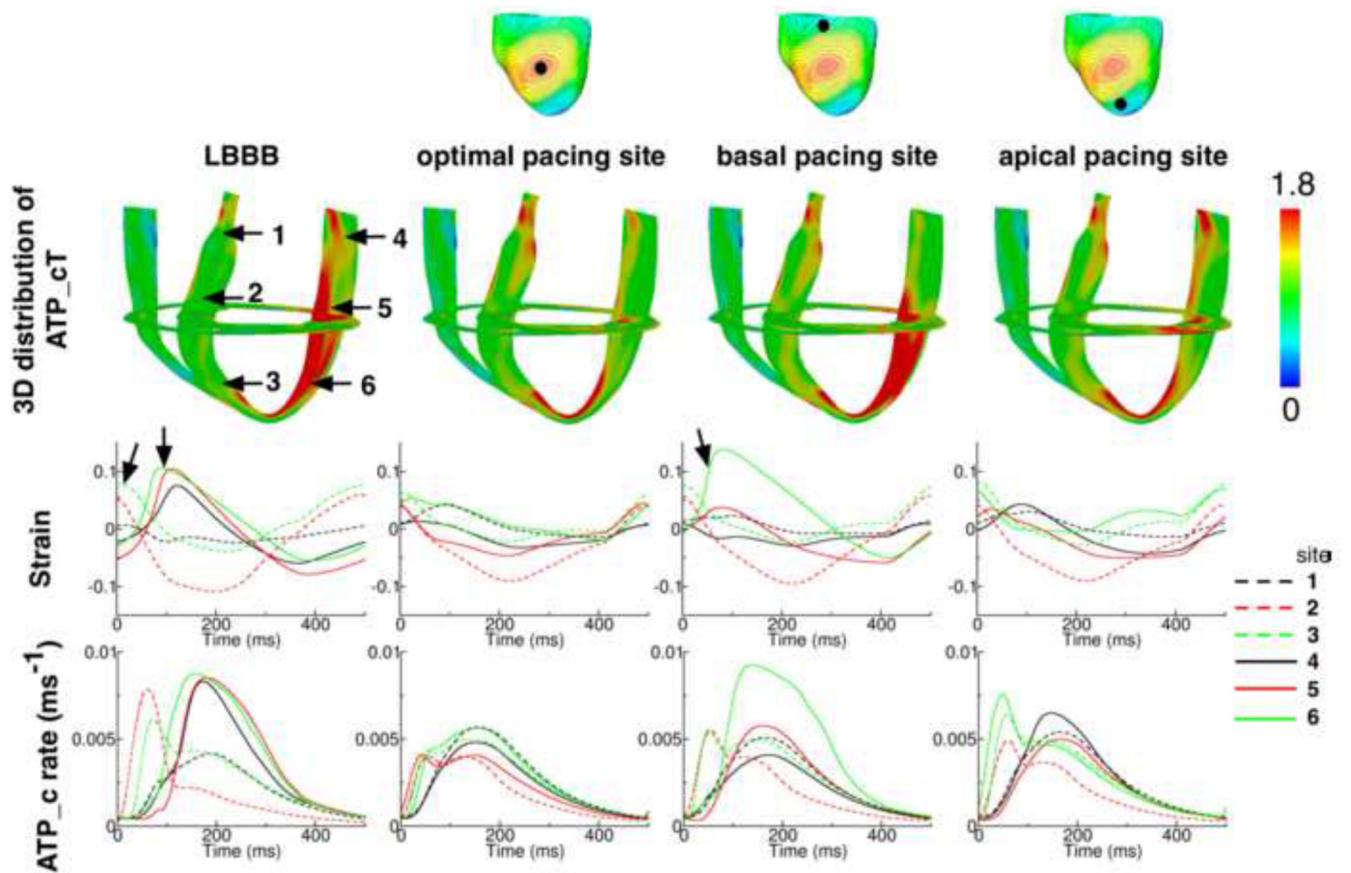


Figure 6.

1st row: Canine ventricles. The black dot indicates the location of the CRT epicardial site from which LV was paced. 2nd row: 3D distribution of ATP_{cT} in the DHF ventricles and the ventricles following CRT from the epicardial LV pacing sites shown in the 1st row. 3rd and 4th rows: Strain and ATP_c profile over one representative pacing cycle at six sites (marked by the arrows in the leftmost image in the 2nd row) from DHF ventricles and following CRT from the epicardial LV pacing sites shown in the 1st row.